



UNIVERSITY OF LEEDS

This is a repository copy of *Effect of evaporator/condenser elevations on a loop heat pipe with non-condensable gas*.

White Rose Research Online URL for this paper:
<https://eprints.whiterose.ac.uk/169105/>

Version: Accepted Version

Article:

Wang, H, Lin, G, Shen, X et al. (3 more authors) (2020) Effect of evaporator/condenser elevations on a loop heat pipe with non-condensable gas. *Applied Thermal Engineering*, 180. 115711. ISSN 1359-4311

<https://doi.org/10.1016/j.applthermaleng.2020.115711>

© 2020, Elsevier. This manuscript version is made available under the CC-BY-NC-ND 4.0 license <http://creativecommons.org/licenses/by-nc-nd/4.0/>.

Reuse

This article is distributed under the terms of the Creative Commons Attribution-NonCommercial-NoDerivs (CC BY-NC-ND) licence. This licence only allows you to download this work and share it with others as long as you credit the authors, but you can't change the article in any way or use it commercially. More information and the full terms of the licence here: <https://creativecommons.org/licenses/>

Takedown

If you consider content in White Rose Research Online to be in breach of UK law, please notify us by emailing eprints@whiterose.ac.uk including the URL of the record and the reason for the withdrawal request.



eprints@whiterose.ac.uk
<https://eprints.whiterose.ac.uk/>

Effect of evaporator/condenser elevations on a loop heat pipe with non-condensable gas

Huanfa Wang¹, Guiping Lin¹, Xiaobin Shen^{1*}, Lizhan Bai¹, Rui Yang¹, Dongsheng Wen^{1,2}

¹ Laboratory of Fundamental Science on Ergonomics and Environmental Control, School of Aeronautic Science and Engineering, Beihang University, Beijing 100191, China

² School of Chemical and Process Engineering, University of Leeds, Leeds, LS2 9JT, UK

Abstract:

The coupling effect of evaporator/condenser elevations and non-condensable gas (NCG) on the performance of a loop heat pipe (LHP) operating in gravitational field was investigated experimentally. Ammonia and nitrogen were selected as the working fluid of LHP and the simulated gas of NCG, respectively. The experiments were conducted at three kinds of evaporator/condenser elevations, namely zero elevation, adverse elevation and positive elevation. Experimental results show that NCG will cause an increase in operating temperature, but the trends varies at different evaporator/condenser elevation elevations. The temperature rises caused by NCG at the zero and adverse elevations are negatively correlated with heat load, and the maximum temperature increments are both at the minimum heat load of 15 W, but the influence of NCG is less at adverse elevation. On the other hand, at favorable elevation, the temperature rise exhibits different characteristics in different LHP operation modes, i.e., positively correlated with heat load in gravity driven mode and negatively in capillarity-gravity co-driven mode, and the transition heat load is 60 W. For an LHP that has already contained a certain amount of NCG, functioning at favorable elevation could eliminate the adverse effects of NCG on operating temperature and heat transfer performance to some extent. Furthermore, it is found that the presence of NCG and adverse elevation appears to inhibit the backflow during startup and improve startup stability. These results might have reference significance for the design and installation of the LHP for terrestrial applications.

Keywords: loop heat pipe; non-condensable gas; evaporator/condenser elevations; steady state characteristics; startup

1. Introduction

Loop heat pipes (LHPs) are two-phase heat transfer devices with high efficiency, and the driving force for the circulation of working fluid is the capillary force generated in the porous wick [1,2]. The evaporation/condensation at the heat source/sink is the basic principle of LHP operation, which is similar to that of heat pipes. As shown in Fig. 1, a complete LHP consists of evaporator, compensation chamber (CC), vapor line, condenser, and liquid line. When a certain heat load is applied to the evaporator, evaporation will occur there with heat absorbed. The evaporant will rush to the condenser through the vapor line and condense into liquid. In this process, the heat is transferred from the evaporator to the condenser. The condensant finally flows back to the CC along the liquid line. The main function of CC is to accommodate the return liquid and adapt to the redistribution of working fluid in the loop. For the purpose of structure compactness, the CC of an LHP is usually integrated with the evaporator as a coupling structure.

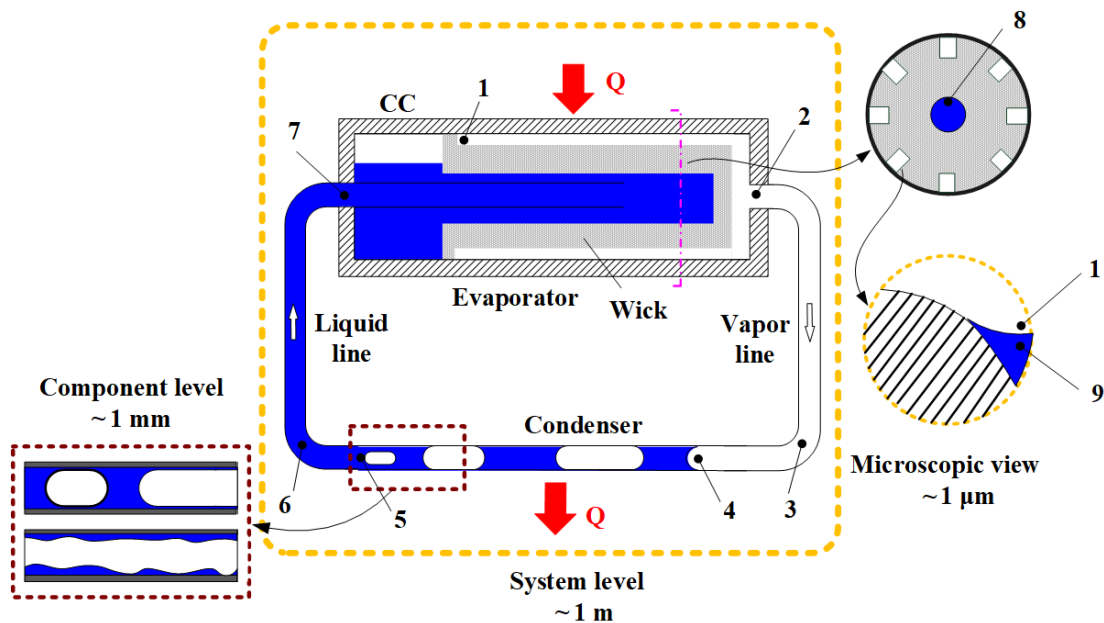


Fig. 1 Schematic of the operating principle of an LHP [3]

Compared with heat pipe, LHP system manifests many additional advantages, including long heat transport distance, installation flexibility and strong adaptability of acceleration field. Thanks to these extraordinary advantages, LHP was first adopted in space applications and successfully applied in the thermal management systems of

many satellites and spacecraft [4–10]. In the last few years, the applications of LHP were extended to the gravitational field gradually and various terrestrial application projects were proposed or successfully practiced, such as aircraft thermal management, anti-icing, as well as heat dissipation of vehicles [11–13]. In short, LHP technology is a promising thermal management solution for terrestrial applications in the future. However, for the terrestrial application of LHPs, there are two key issues that need to be solved urgently, namely the effects of gravity and non-condensable gas (NCG).

An important feature of the LHP operating in the gravitational field is that its operation will inevitably be affected by the space attitude (i.e. the relative height between components), which is quite different from the case in space microgravity environment [14]. The space attitude of an LHP with cylindrical evaporator mainly includes two types, namely the tilt of evaporator and the elevation of evaporator/condenser. The tilt of evaporator changes the relative height of evaporator and CC, which affects the liquid-vapor distribution and heat transfer in CC. Since the operating temperature is usually determined by the energy balance of CC [1], the evaporator tilt will eventually have a significant impact on the LHP operating characteristics, as reported by Ref [15]. Besides, the elevation of evaporator or condenser also has a great effect on the LHP operation because of the action of liquid head in the gravitational field [14,16]. Compare to the case where the evaporator and condenser are at the same height (i.e. zero elevation), adverse elevation means that the evaporator is raised, which increases the flow resistance and adversely affects the operation (i.e. operating temperature increase). Conversely, when the condenser is higher than the evaporator, this kind of elevation is advantageous for LHP operations (i.e. operating temperature decrease) and could be called favorable elevation.

The NCG in a two-phase heat transfer system is the gas impurity that remains in a gas state throughout the operating temperature range of a device and cannot be condensed into a liquid state. In the last twenty years, studies have confirmed that the presence of NCG in the system is a momentous reason for the performance degradation and life-span shortening of LHPs [17–25]. In general, for an LHP operating in space, the generation of NCG can only be attributed to the chemical reaction between working

fluid and LHP casing. As the service time increases, the amount of NCG will accumulate gradually. However, even though chemically compatible materials and rigorous cleaning processes were adopted in the manufacturing process, suspected NCG-induced LHP failure cases still occur occasionally [26,27]. Thus, we have reason to believe that the existence of NCG in an LHP system is almost inevitable. When the LHP is transferred from space to the ground, the underlying factors that cause NCG generation will not disappear and the NCG problem will be inherited into the terrestrial application. In addition, different from the vacuum environment in the universe, there is an atmosphere on the surface of the earth and terrestrial application means that the LHP system will be exposed to an air-filled environment directly. On account of the imperfection of sealing technology, it is reasonable to imagine that the possibility of air entering the loop will increase greatly, especially when the operating pressure of working fluid is lower than the ambient pressure. Therefore, compared with space applications, LHP for terrestrial applications is more likely to encounter NCG problems.

Obviously, the LHP for terrestrial applications has a considerable possibility of encountering the effects of NCG and space attitude simultaneously. And for the purpose of reliability, it is essential to investigate the coupling effect of space attitude and NCG systematically. However, from the literature review, although the impact of NCG on the performance of LHP has been studied in depth, most studies were based on a fixed LHP attitude, typically zero elevation with no evaporator tilt. So far, only a few studies have explored the effect of NCG at adverse elevation deficiently [25,28], but no studies have involved the favorable elevation. Therefore, the coupling effect of the two factors are still not clear enough and a systematic research is urgently needed. In our previous study, the coupling effect of evaporator tilt and NCG has been studied experimentally, and some interesting conclusions have been drawn, such as the temperature increment caused by NCG seems to be the smallest at adverse tilt [21]. From this point, our research direction would turn to the elevation of evaporator or condenser, which composed the main content of this article.

2. Experimental setup

2.1. Description of the experimental system

A three-dimensional view of the tested LHP was displayed in Fig. 2 and the basic parameters and detailed description of different LHP components were listed in Table 1. The evaporator and CC of the LHP was cylindrical, and the internal structure of the evaporator-CC assembly was shown in Fig. 3 in the form of a three-dimensional diagram. The casing of the LHP was manufactured by stainless steel 304. And in view of the wide application and chemical compatibility, ammonia was chosen as the working fluid. The primary wick was sintered by nickel powder. The outer surface of the primary wick was machined with eight rectangular channels for the removal of vapor, and a blind hole was drilled in the center of the wick as the evaporator core. The bayonet tube was connected with the liquid line, and its outlet was extended to the vicinity of the bottom of the evaporator core hole. Some SS-304 wire meshes were welded on the bayonet tube and filled in the evaporator core as the secondary wick to enhance the stability of liquid supply. For the purpose of clarity, the secondary wick was not shown in Fig. 3.

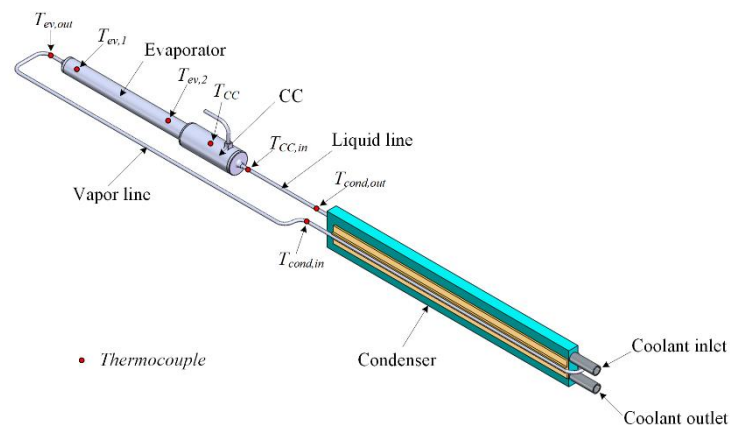


Fig. 2 Three-dimensional view of the LHP and thermocouple locations

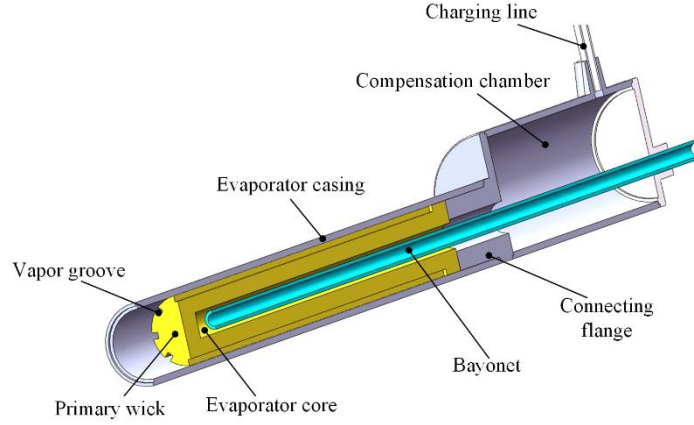


Fig. 3 Three-dimensional cross-section view of the evaporator-CC assembly

Table 1 Detailed description of the LHP components

Component	Material and description
Evaporator casing ($D_o \times D_i \times L$)	SS-304 ($\Phi 13\text{mm} \times \Phi 11\text{mm} \times 130\text{mm}$)
Primary wick ($D_o \times D_i \times L$)	Nickel ($\Phi 11\text{ mm} \times \Phi 4\text{ mm} \times 100\text{ mm}$) with porosity of $\sim 55.0\%$ and maximum pore radius $\sim 1.0\text{ }\mu\text{m}$
Secondary wick	SS-304 wire mesh with average pore radius of $\sim 20\text{ }\mu\text{m}$
Bayonet ($D_o \times D_i \times L$)	SS-304 tube ($\Phi 3\text{ mm} \times \Phi 2\text{ mm} \times 163\text{ mm}$)
Vapor line ($D_o \times D_i \times L$)	SS-304 tube ($\Phi 3\text{ mm} \times \Phi 2\text{ mm} \times 1160\text{ mm}$)
Condenser line ($D_o \times D_i \times L$)	SS-304 tube ($\Phi 3\text{ mm} \times \Phi 2\text{ mm} \times 1200\text{ mm}$)
Liquid line ($D_o \times D_i \times L$)	SS-304 tube ($\Phi 3\text{ mm} \times \Phi 2\text{ mm} \times 900\text{ mm}$)
Compensation chamber (including the connecting flange)	SS-304 with volume of 15.26 ml
Working fluid (m)	Ammonia ($11.0 \pm 0.1\text{ g}$) with purity of 99.999%

The schematic diagram of experimental system was shown in Fig. 4. A kapton heater with a nominal resistance of 20.5Ω was attached on the evaporator casing by double-faced adhesive. The size of the kapton heater was specially designed as $41 \text{ mm} \times 100 \text{ mm} \times 0.1 \text{ mm}$ (length \times width \times thickness), which could match the size of primary wick perfectly and the heat flux applied on the primary wick could be considered as uniform. As the resistance of kapton heaters would increase with the rise of temperature, the uncertainty of heater resistance was determined experimentally as 0.81% in the temperature range of 20-120 °C. The kapton heater was connected to a DC power supply (PSW 160-21.6, Good Will Instrument Co., Ltd) and the output current could be controlled with a maximum uncertainty of 0.1%. Then, the heating power of the kapton heater could be calculated by Joule's law with an uncertainty of about 0.83%.

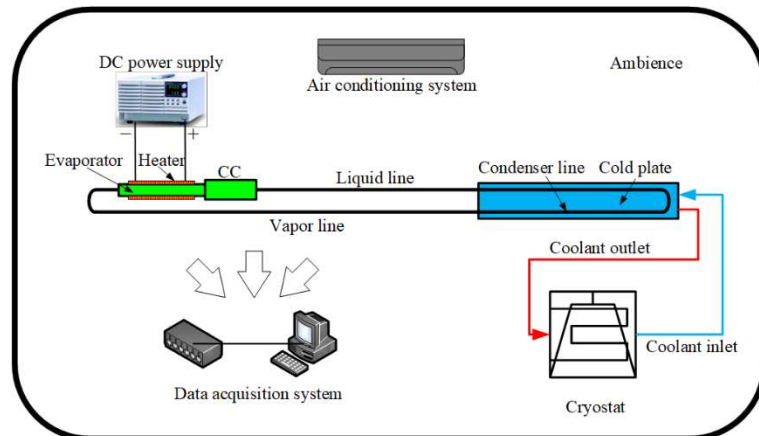


Fig. 4 Schematic diagram of the experimental system

As displayed in Fig. 2, the condenser line was welded to two pieces of slotted copper plates which were attached to an aluminum cold plate. The contact surface of copper plate and cold plate was filled with a thin layer of high-performance thermal grease (GD900, Foshan High Conductivity Electronic Co., Ltd., China) to minimize the contact thermal resistance. The cold plate of the condenser was cooled by a cryostat (Sanffo Limited, China) with water as the coolant fluid. The average volume flow rate of the coolant was 3.75 L/min, which was measured by a flowmeter (FHKU 938-1530/F01, Digmesa AG, Switzerland) with a measuring accuracy of $\pm 2.0\%$. The temperature of the coolant in the cryostat could be controlled with a maximum error of

± 0.5 °C and the heat sink temperature could be recognized as constant.

The temperature at different locations of the LHP was measured with the help of T-Type thermocouples (TT-T-30, Omega Engineering, USA). The schematic of the thermocouple locations was illustrated in Fig. 2 and these locations included evaporator casing, evaporator outlet, condenser inlet/outlet, the top of CC, as well as the ambience. The thermocouples were calibrated with the method of thermostatic water bath and the maximum uncertainty was ± 0.46 °C.

The evaporator, compensation chamber, transport lines (including vapor and liquid lines), condenser, as well as the coolant pipeline were covered by 10 mm thick rubber foam insulation material, of which the thermal conductivity was about 0.034 W/(m·K). The temperature data measured by the thermocouples was recorded by a personal computer with the help of a set of Agilent 34970A Data Acquisition/Switch Unit (with Agilent 34901A multiplexer cards and Agilent Benchlink Data Logger 3 software). The time interval between each data collection and recording was 5 s. The ambient temperature was controlled by an air conditioning system with a maximum uncertainty of ± 2 °C.

2.2. Experimental conditions and procedure

A summary of the experimental conditions was shown in Table 2. As summarized in Section 1, the impact of NCG on the operation of an LHP operated at zero elevation had been studied extensively, and thus was not the main object of this study. However, the zero-elevation experiment was the baseline for comparison and analysis, which should be conducted necessarily under current experimental settings. A schematic of the various evaporator/condenser elevations was illustrated in Fig. 5. It should be noted that the tilt angles of the evaporator and the condenser were both set to 0 ° in consideration of control variables. As given in Table 1, the transport line was made of metal tubes with small diameter, which could be bent easily to meet the spatial attitude requirement above. The symbol ΔH represented the absolute value of the height difference between the evaporator and the condenser, and the maximum uncertainty was about ± 0.02 m.

Table 2 Summary of the experimental conditions

Variable	Description and value
Evaporator/condenser elevation	Zero elevation ($\Delta H=0$ m)
	Adverse elevation ($\Delta H=0.5$ m)
	Favorable elevation ($\Delta H=0.5$ m)
NCG inventory ($\times 10^{-5}$ mol)	0
	2
Heat load (W)	15, 30, 45, 60, 75, 90, 105, 120, 135
Heat sink temperature ($^{\circ}\text{C}$)	20

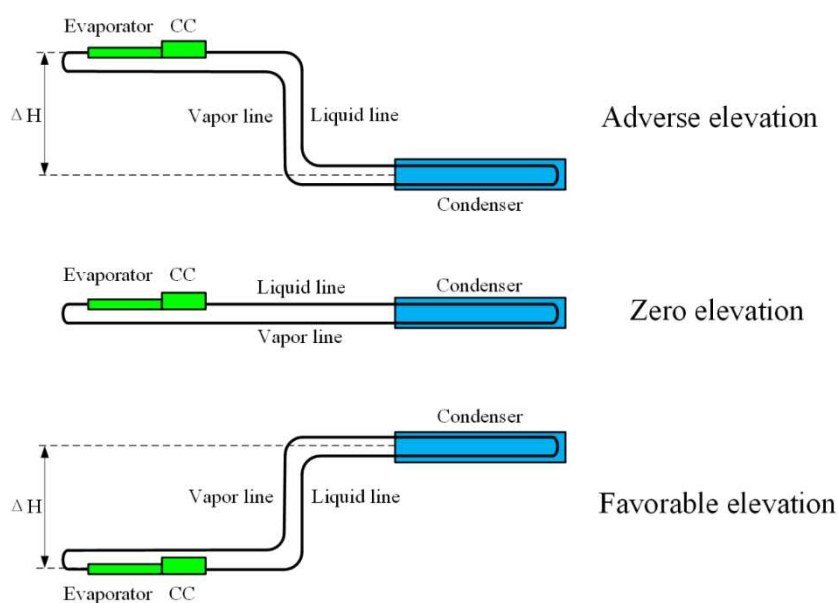


Fig. 5 Schematic of the various evaporator/condenser elevations

To minimize the residual NCG in the loop at the initial state pipeline, strict cleaning procedure had been conducted before the working fluid was charged. After the experiment without NCG was completed, nitrogen with a purity of 99.995% was injected into the loop to simulate the NCG in the system. The injection of NCG was completed with the help of a set of NCG injection system as shown in the Fig. 6, and the maximum charging error was about $\pm 3\%$. More detailed experimental procedure was introduced in our previous study [21] and would not be repeated here.

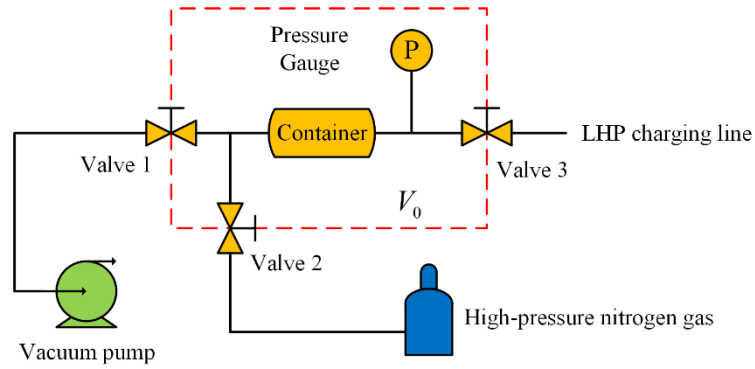


Fig. 6 Schematic of the NCG injection system

3. Results and Discussion

3.1. Steady state characteristics

When the LHP operated at a steady state, the saturation temperature was a critical characterization of the performance. Since the working fluid in CC was at a two-phase state, the temperature at the top of CC could be considered as the saturation temperature of the LHP. Besides, the temperature of vapor in the vapor line was also usually chosen as a description of the steady state characteristics, which could reflect the maximum temperature of the working fluid in the loop.

As shown in Fig. 7 and Fig. 8, when the LHP operated at zero elevation, the maximum saturation temperature and the vapor temperature were 28.9 °C and 31.5 °C respectively, and the LHP displayed good temperature control characteristics within the whole heat load range. After the injection of NCG, both the saturation temperature and the vapor temperature increased significantly, especially when the heat load was relatively small. The maximum increment of saturation temperature and vapor temperature were 6.8 °C and 6.6°C respectively, which was observed at the minimum heat load of 15 W. As the heat load increased, the temperature increment caused by NCG went down, and the minimum values, which were achieved at a heat load of 135 W, were only 1.2 °C and 3.7 °C for the saturation and vapor temperatures respectively.

The reasons that the injection of NCG would lead to a temperature rise of LHP operated at zero elevation had been analyzed in the previous studies [19,21] and a brief summary would be conducted here. It was generally acknowledged that the temperature of CC (i.e. saturation temperature) was positively correlated with the heat leak from evaporator to CC. As a result of the pressure distribution in the loop, the injected NCG

would accumulate in CC and produce a partial pressure, which increased the pressure difference between evaporator and CC. Considering the operation principle of LHP, the heat leak would increase by reason of thermo-hydraulic linkage among various components of LHP, leading to a temperature rise in CC and further the vapor temperature at the evaporator. As the heat load increased, the mass flow rate of the liquid back to CC would increase and produce a better cooling effect to balance the increased heat leak. Therefore, the adverse effect of NCG would be attenuated at high heat loads.

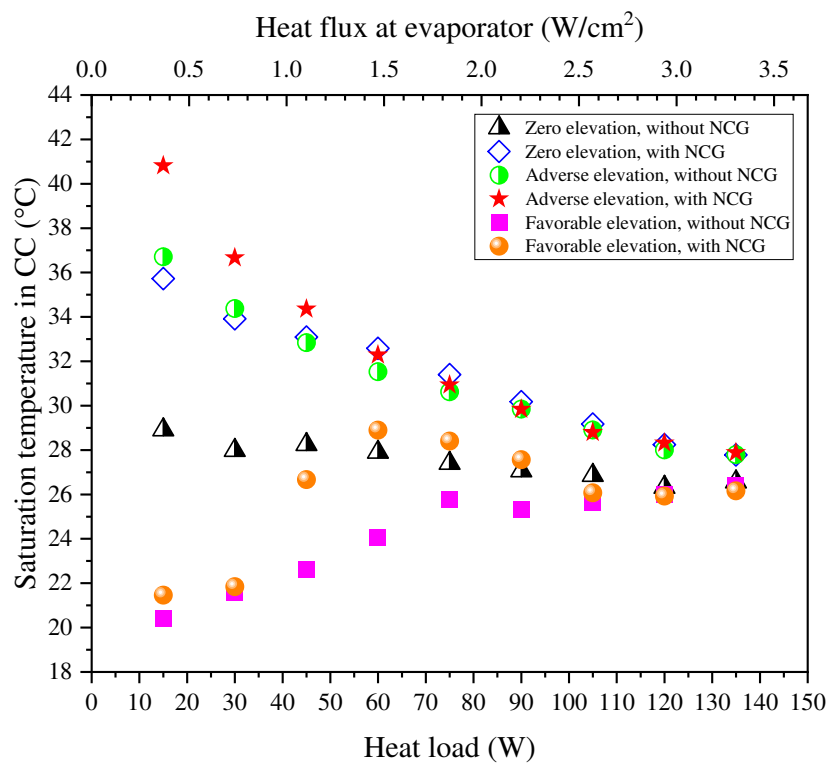


Fig. 7 Comparison of effects for NCG and different evaporator/condenser elevations on saturation temperature in CC

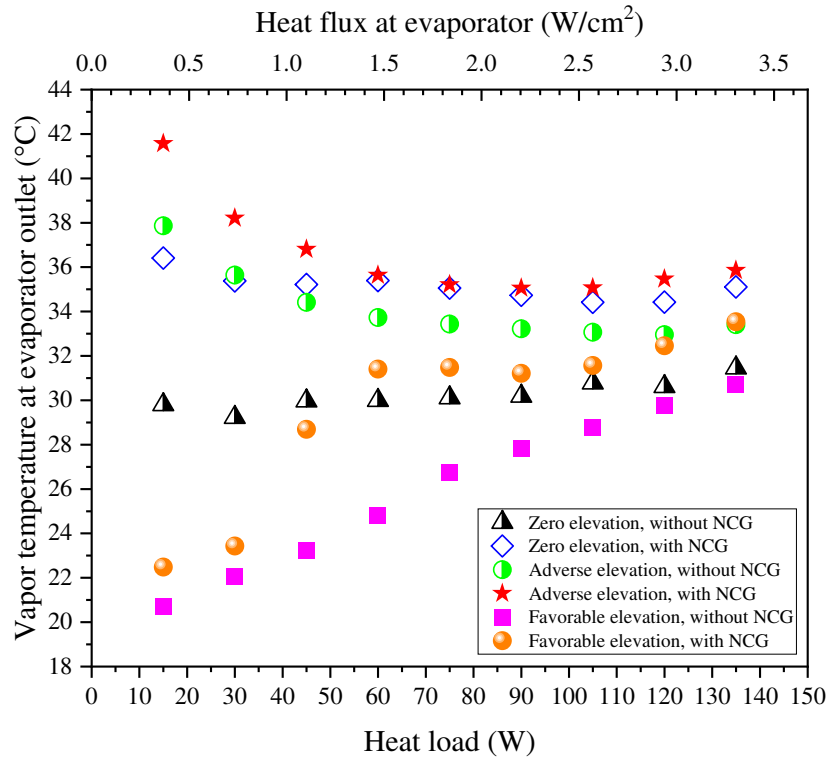


Fig. 8 Comparison of effects for NCG and different evaporator/condenser elevations on vapor temperature at evaporator outlet

When the space attitude of the LHP changed from zero elevation to adverse one, it could be inferred from the operation principle of LHP that the injection of NCG would also lead to the temperature rises and the experimental results confirmed this inference. As shown by Fig. 7, the rise of the saturation temperature in CC was at a value of 4.1 °C when the heat load was 15 W, and decreased continuously as the heat load increased. However, different from the case at zero elevation, the temperature rise caused by NCG was quite small. Especially when the heat load was larger than 75 W, the temperature rise at CC was negligible considering the measurement error of the thermocouples. Besides, as displayed by Fig. 8, the temperature rise of the vapor at the evaporator outlet was about 2.7 ± 1.0 °C within the whole heat load range, which was also smaller than the case at zero elevation.

Another important phenomenon was that when the LHP was operated in the two cases of “zero elevation & with NCG” and “adverse elevation & without NCG”, the saturation temperatures in CC were almost the same, as shown in Fig. 7. This means that a 2×10^{-5} mol NCG injection and 0.5 m adverse elevation produced similar effects

on the steady state operation under the current experimental settings. Actually, the liquid gravity head introduced by adverse elevation increased the flow resistance in the loop and further the pressure difference between evaporator and CC. Since the mechanisms of NCG and adverse elevation were consistent to some extent, the negative impact on temperature was qualitatively superimposable if an LHP suffered from adverse elevation and NCG accumulation simultaneously. However, it should be noted that this superposition was numerically non-linear due to variations in the physical properties of the working fluid and NCG. As shown by Fig. 9, the temperature rise caused by the simultaneous action of NCG and adverse elevation was less than the sum of the temperature rises caused by the separate actions of the two factors.

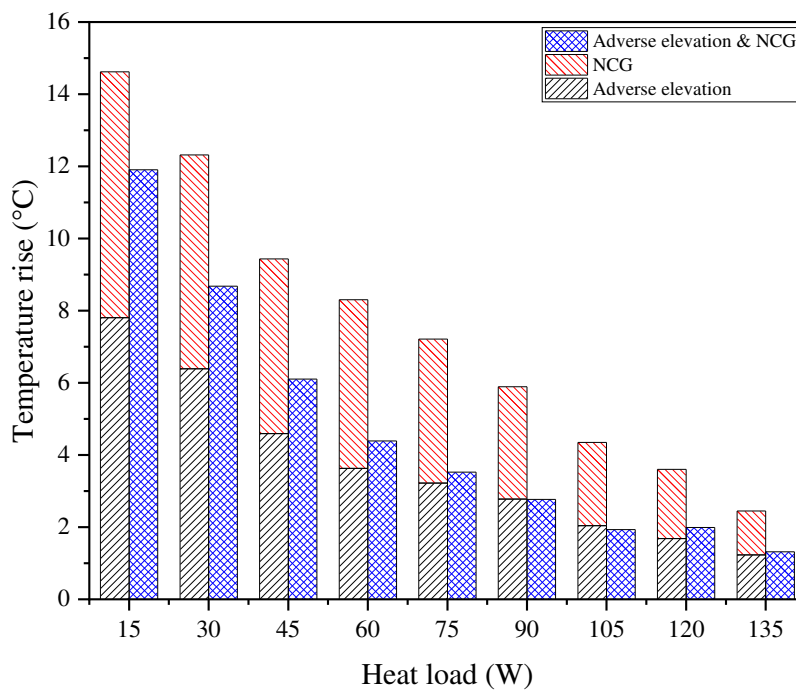


Fig. 9 Comparison of saturation temperature rises caused by adverse elevation and/or NCG

When the LHP was functioning at favorable elevation, the induction of NCG also led to an increase in saturation temperature and vapor temperature, as shown in Fig. 7 and Fig. 8. However, the heat load dependence of the temperature rise displayed quite different characteristics. The maximum rise of saturation temperature and vapor temperature resulting from the injection of NCG was observed at 60 W, and the values

were about 4.8 °C and 6.6 °C, respectively. When the heat load was lower than 60 W, the temperature rise was positively correlated with the heat load, and when the heat load exceeded 60 W, the temperature rise decreased gradually as the heat load increased. Especially when the heat load was larger than 105 W, the rise of saturation temperature could be neglected within the measurement error range.

The reason for this phenomenon could be attributed to the fact that the working principle of LHP operating at favorable elevation was not unique. According to Ref [29–31], depending on the magnitude of heat load, the LHP could operate in two different modes, namely gravity driven mode and capillarity-gravity co-driven mode. The working principle (Pressure vs. temperature diagram) of the two modes could be seen in Fig. 10. When the heat load was relatively small, the LHP worked in gravity driven mode. In this mode, no capillary force was generated in the wick, and the gravity difference between the working fluid in liquid line and vapor line was sufficient to act as the only driving force. But when the heat load applied to the evaporator increased, the circulation in the loop was no longer driven separately by gravity difference due to the growing up of flow resistance in the loop. At this moment, capillary force developed in the porous wick would serve as a part of the driving force and the operation mode turned into capillarity-gravity co-driven mode. In the experiment, the heat load with a value of 60 - 75 W could be roughly considered as the critical heat load at which the transition occurred between the two operating modes.

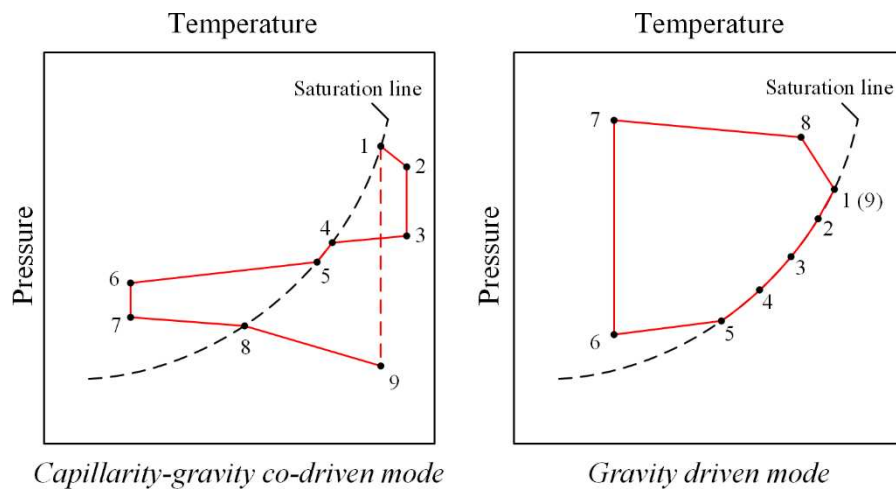


Fig. 10 Pressure vs. temperature diagram of an LHP operating in capillarity-gravity co-

driven mode and gravity driven mode (not to scale). The corresponding relationship between Numbers and locations is shown in Fig. 1.

When the LHP operated at capillarity-gravity co-driven mode, that is, the heat load was larger than 60 W the operation principle was almost the same as the case at zero elevation or adverse elevation. The vapor pressure of CC would be the lowest in the entire loop and the NCG would be gathered here. The mechanism by which the NCG caused an increase in temperature was the same and had been analyzed before. Hence, the temperature rise would decrease with the augmentation of heat load.

However, the operation principle of an LHP worked in gravity driven mode was quite different. In this case, the LHP worked like a loop thermosyphon and the working fluid in vapor line was usually in a two-phase saturated state and condensed into liquid in condenser gradually [31,32]. As the working fluid was circulated by the gravitational pressure difference between the liquid line and vapor line, the condenser would become the lowest point of vapor pressure in the system and the NCG would be mainly distributed here consequently. Different from the NCG accumulated in CC, the NCG in the condenser will significantly reduce the effective heat transfer area and thus lead to a reduction of the heat transfer capacity eventually. Hence, the increase in the LHP temperature in gravity driven mode was due to the reduction in condenser efficiency caused by the block of NCG. The influence of NCG on temperature in this mode could be qualitatively concluded by the formula

$$T_{2\phi} = T_{cond} = \frac{Q}{(hA)_{cond}} + T_{sink} \quad (1)$$

And Eq. (1) could be written in differential form, namely

$$dT_{2\phi} = -\frac{Q}{(hA)_{cond}^2} d(hA)_{cond} \quad (2)$$

As shown by Eq. (2), $dT_{2\phi}$ was positively correlated with heat load. This means that the temperature rise caused by NCG will increase as the heat load going up, which is consistent with the experimental results.

Fig. 11 is a comparison of saturation temperature changes caused by favorable elevation and/or NCG. When the LHP is operating in gravity driven mode, the effect of

favorable elevation dominates and the adverse effect of NCG are weakened greatly. As the heat load increases, the operating of LHP will switch to capillarity-gravity co-driven mode gradually and the favorable elevation will lose its dominant position. The coupling effect of NCG inventory and favorable elevation on operating temperature gradually shifts from a negative effect to approximate zero effect. This indicates that when the LHP works in capillarity-gravity co-driven mode under the current experimental settings, the adverse effect of 2×10^{-5} mol NCG inventory could be offset approximately by a favorable elevation of about 0.5 m. In fact, this result could be expected since the adverse effect of 2×10^{-5} mol NCG inventory is similar to that of 0.5 m adverse elevation. This is because the presence of favorable elevation reduces the flow resistance, which in turn compensates for the increased pressure difference between the evaporator and CC caused by the NCG partial pressure.

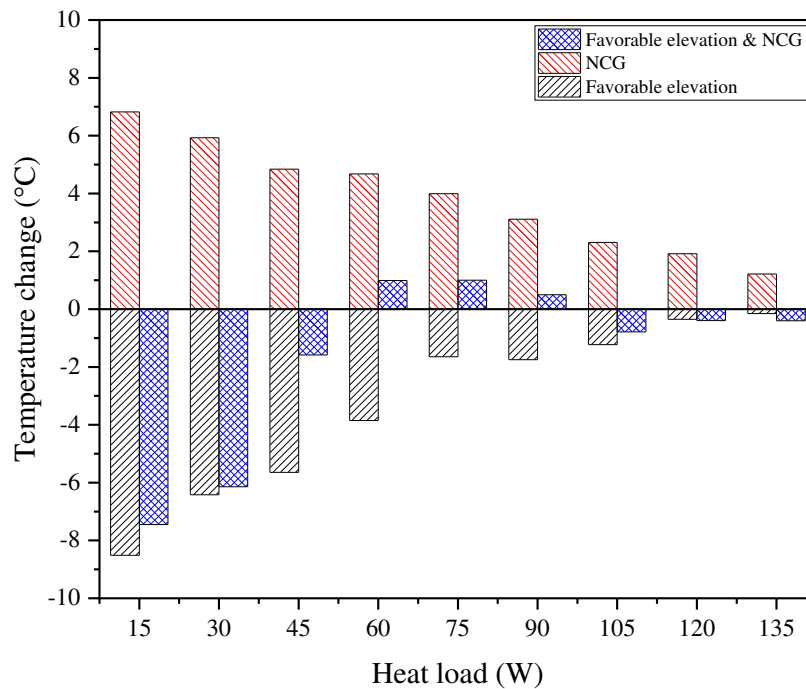


Fig. 11 Comparison of saturation temperature changes caused by favorable elevation and/or NCG

The thermal resistance of condenser was considered as an important measurement of the steady state thermal characteristic of an LHP. The calculation method of condenser thermal resistance could be shown by Eq. (3) and the results were illustrated

by Fig. 12.

$$R_{cond} = \frac{T_{CC} - T_{sink}}{Q} \quad (3)$$

When the LHP is functioning in zero elevation or adverse elevation, the condenser thermal resistance would decrease gradually as the heat load increases, whether NCG is injected or not. The injection of NCG would lead to a significant increase in the condenser thermal resistance at a relatively small heat load. At high heat loads, the corresponding value tends to exhibit consistency and stability, which is about 0.05 °C/W. The effects of NCG and adverse elevation on condenser thermal resistance could be negligible under a sufficiently large heat loads. However, at a favorable elevation, the condenser thermal resistances would always be relatively small. The maximum values are calculated as 0.148 °C/W and 0.077 °C/W in the cases with and without NCG, respectively. The maximum values of the condenser thermal resistance are observed near the transition heat load of gravity driven mode and capillarity-gravity co-driven mode, which is about 60W and 75 W for the cases with and without NCG. In addition, when the heat load is large enough, the condenser thermal resistance also tends to be stable under favorable elevation, and the calculated value is almost the same as that under zero and adverse elevation, which is about 0.05 °C/W. These results show from another perspective that the influence of NCG and favorable/adverse elevation on the heat transfer performance of an LHP is mainly manifested under small heat loads, and when the heat load is sufficiently large, the effect is quite small.

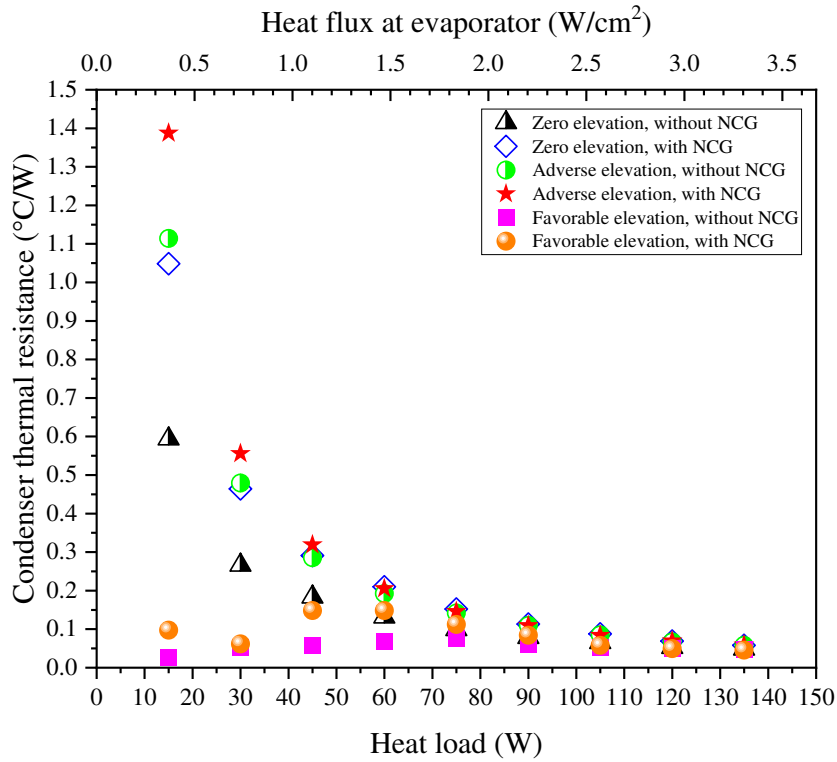


Fig. 12 Comparison of effects for NCG and different evaporator/condenser elevations on condenser thermal resistance

3.2. Backflow phenomenon during startup

The LHP in a shutdown state will undergo a startup process after a certain heat load is applied to the evaporator. If the LHP is able to reach a steady state operation and the maximum temperature is within the permissible range, we can believe that the startup is successful. Judging from this standard, all the startups in this experiment could be considered as successful.

Fig. 13 was a representative startup process obtained in this study, which demonstrated the temperature changes from the application of heat load to the steady state. After the evaporator was heated, the temperature of evaporator casing (i.e. $T_{ev,1}$ and $T_{ev,2}$) increased quickly and the temperature at evaporator outlet (i.e. $T_{ev,out}$) was observed to rise sharply. This indicated that evaporation occurred on the outer surface of wick and the generated vapor flowed into the vapor line. As the evaporation continued, the vapor began to enter the condenser and an increase in the condenser inlet temperature (i.e. $T_{cond,in}$) could be observed. Finally, the liquid with low temperature

would flow out of the condenser and enter the CC to balance the heat leak from evaporator to CC. This flow process corresponded to the temperature changes of $T_{cond,out}$ and $T_{CC,in}$. At this point, the circulation of the working fluid was basically established and the operation of the LHP would reach a steady state gradually.

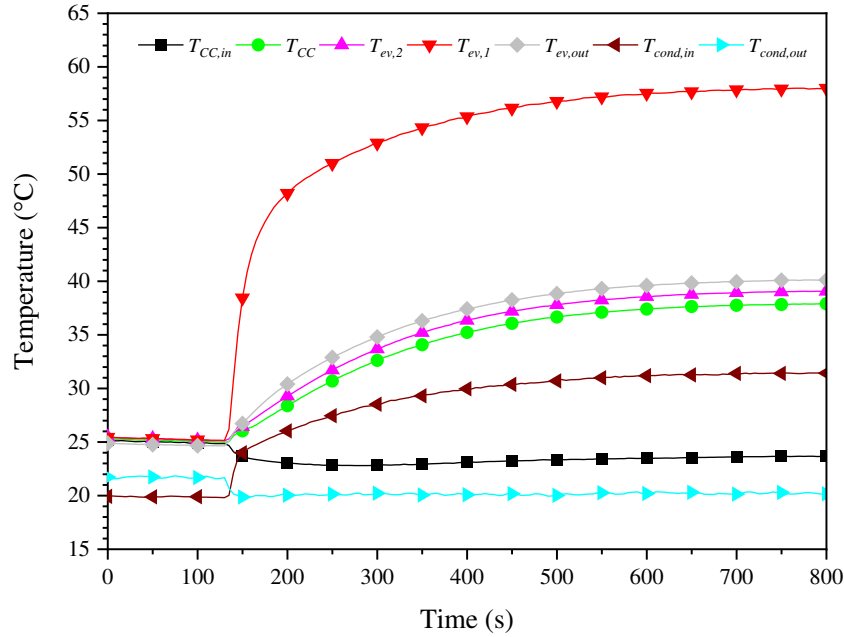


Fig. 13 A representative startup process obtained in this study (Q=45 W, zero elevation, with NCG)

It should be noted that the saturation temperature in CC (i.e. T_{CC}) increased just after the evaporator was heated. This means that the heat leak from evaporator to CC was relatively large. As a matter of fact, all the startup tests conducted in this study were accompanied by this feature, which might indicate that there was a liquid-vapor interface in CC prior to startup.

Sometimes, the heat leak from the evaporator to CC could be quite large for some reasons, such as vapor penetrating the wick into CC, resulting in a rapid rise of the CC temperature. Since the working fluid in CC was at a saturation state, the pressure and the temperature in CC were coupled to each other according to the Clapyron-Clausius equation. As the temperature rose, the pressure at CC would also increase, even exceeding the pressure at evaporator. At this point, the working fluid in CC would flow

along the transport lines to the evaporator and a “backflow” phenomenon occurred.

As shown in Fig. 14, the temperature at CC inlet (i.e. $T_{CC,in}$) suffered from a sharp rise just after the increase of T_{CC} , indicating that the fluid with high temperature in CC entered the liquid line. In general, the backflow was temporary and would disappear as the temperature continued to rise, as shown in Fig. 14. However, if the backflow still existed before the evaporator temperature exceeded the limit, a startup failure could be suffered from. In summary, although all the startups in this study were successful, it is still believed that the backflow phenomenon occurred was a signal that the startup was not robust enough.

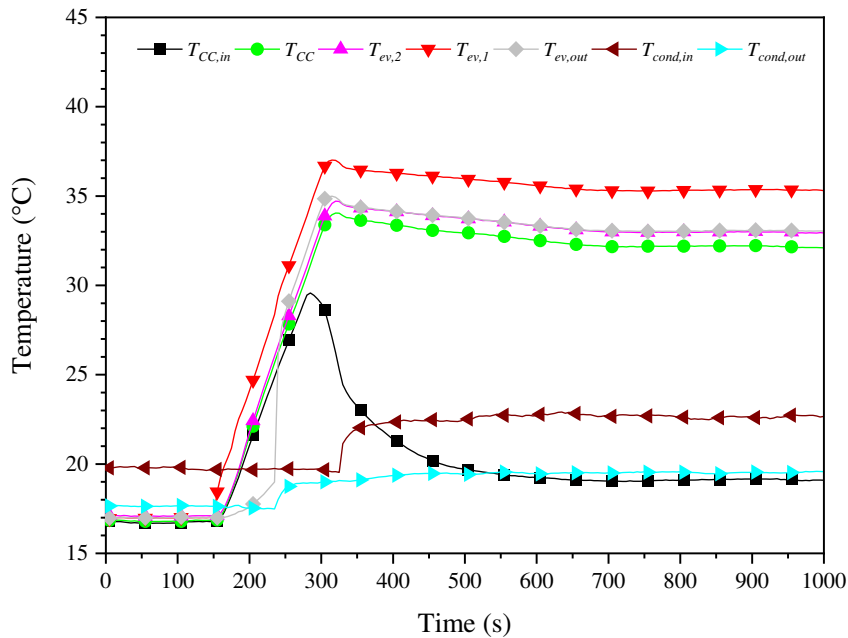


Fig. 14 Startup process with backflow (Q=15 W, zero elevation, without NCG)

In order to investigate the effects of evaporator/condenser elevations and NCG on the backflow phenomenon during LHP startup, a series of startup tests were carried out and the results were displayed in Table 3. By analyzing the results, it seems that the introduction of adverse elevation and NCG has a certain inhibitory effect on the backflow phenomenon during startup. However, it is unfortunate that the startup of an LHP is a complicated thermodynamic process accompanied by phase change and phase movement, and besides, the existence of NCG further increases the complexity [33]. In

addition, the specific startup pattern of an LHP usually has a certain randomness and thus a large number of startup tests are needed for statistical analysis. For the reasons above, we have not got a very convincing explanation about this phenomenon yet and more in-depth research needs to be carried out in the future to draw a clearer conclusion.

Table 3 Summary of the backflow phenomenon during startup (\checkmark : with backflow \times : without backflow)

Experimental conditions		Startup heat load (W)				
		15	45	75	105	135
Zero elevation	Without NCG	\checkmark	\checkmark	\checkmark	\checkmark	\checkmark
	With NCG	\checkmark	\times	\times	\times	\times
Adverse elevation	Without NCG	\checkmark	\times	\times	\checkmark	\times
	With NCG	\times	\times	\times	\times	\times
Favorable elevation	Without NCG	\checkmark	\checkmark	\checkmark	\checkmark	\checkmark
	With NCG	\checkmark	\times	\times	\times	\checkmark

4. Conclusions

This study investigated the effects of three different evaporator/condenser elevations (i.e. zero elevation, adverse elevation and favorable elevation) on the steady state and startup performance of an LHP containing a certain amount of NCG. The main conclusions could be summarized as follows:

- (1) NCG will lead to an increase in the steady state temperature of LHP at all the three kinds of the evaporator/condenser elevations.
- (2) The temperature rise caused by NCG is negatively correlated with heat load when the LHP operates at zero and adverse elevation. The temperature rises reach their maxima both at 15 W, and the saturation temperature increments are 6.8 °C for zero elevation and 4.1 °C for adverse elevation.
- (3) Under favorable elevation, the temperature rise caused by NCG exhibits different characteristics in different LHP operation modes, i.e., positively correlated with heat load in gravity driven mode and negatively in capillarity-gravity co-driven mode. The maximum rise of the saturation temperature is 4.8 °C at the heat load of 60W.
- (4) The negative influence on temperature is qualitatively superimposable if an LHP

suffered from adverse elevation and NCG accumulation simultaneously, but the temperature rise caused by NCG under adverse elevation is usually smaller than that under zero elevation.

(5) For an LHP that has already contained a certain amount of NCG, functioning at favorable elevation could eliminate the adverse effects of NCG on operating temperature and heat transfer performance to some extent.

(6) The impact of evaporator/condenser elevations and NCG on the startup procedure is very complex, but to some extent, the presence of NCG and adverse elevation appears to inhibit the backflow phenomenon during the startup and improve the startup stability.

Conflicts of Interest

Author declares that there is no conflict of interest

Acknowledgments

This work was supported by the National Natural Science Foundation of China (No. 51576010).

Nomenclature

A Area [m^2]

h Convective heat transfer coefficient [W/m^2]

Q Heat load [W]

R Thermal resistance [$^{\circ}\text{C}/\text{W}$]

T Temperature [$^{\circ}\text{C}$]

Subscripts

2ϕ Two phase

$cond$ Condenser

ev Evaporator

in Inlet

out Outlet

$sink$ Heat sink

References

[1] J. Ku, Operating characteristics of loop heat pipes, SAE Tech. Pap. (1999) 16.

- doi:10.4271/1999-01-2007.
- [2] Y.F. Maydanik, Loop heat pipes, *Appl. Therm. Eng.* 25 (2005) 635–657.
doi:10.1016/j.applthermaleng.2004.07.010.
- [3] H. Wang, G. Lin, L. Bai, J. Fu, D. Wen, Experimental study on an acetone-charged loop heat pipe with a nickel wick, *Int. J. Therm. Sci.* 146 (2019) 106104. doi:10.1016/j.ijthermalsci.2019.106104.
- [4] W. Larson, J. Wertz, Space mission analysis and design, *Choice Rev. Online.* 29 (1992) 29-5149-29–5149. doi:10.5860/choice.29-5149.
- [5] K. Goncharov, O. Golovin, V. Kolesnikov, Zhao Xiaoxiang, Development and flight operation of LHP used for cooling nickel-cadmium batteries in Chinese meteorological satellites FY-1, in: *13th Int. Heat Pipe Conf. Vol.1* 13th, 2004.
- [6] G. Wang, D. Mishkinis, D. Nikanpour, Capillary heat loop technology: Space applications and recent Canadian activities, *Appl. Therm. Eng.* 28 (2008) 284–303. doi:10.1016/j.applthermaleng.2006.02.027.
- [7] E.W. Grob, Mission performance of the GLAS thermal control system - 7 years in orbit, *40th Int. Conf. Environ. Syst. ICES 2010.* (2010) 1–19.
- [8] J.I. Rodriguez, A. Na-Nakornpanom, In-flight performance of the TES loop heat pipe heat rejection system - Seven years in space, *42nd Int. Conf. Environ. Syst. 2012, ICES 2012.* (2012) 1–10. doi:10.2514/6.2012-3500.
- [9] R.R. Riehl, Heat pipes and loop heat pipes acceptance tests for satellites applications, *AIP Conf. Proc.* 1103 (2009) 82–90. doi:10.1063/1.3115582.
- [10] H. Zhang, M. Mi, J. Miao, L. Wang, Y. Chen, T. Ding, X. Ning, Y. Huo, Development and on-orbit operation of loop heat pipes on chinese circumlunar return and reentry spacecraft, *J. Mech. Sci. Technol.* 31 (2017) 2597–2605.
doi:10.1007/s12206-017-0501-x.
- [11] C. Zilio, G. Righetti, S. Mancin, R. Hodot, C. Sarno, V. Pomme, B. Truffart, Active and passive cooling technologies for thermal management of avionics in helicopters: Loop heat pipes and mini-Vapor Cycle System, *Therm. Sci. Eng. Prog.* 5 (2018) 107–116. doi:10.1016/j.tsep.2017.11.002.

- [12] Q. Su, S. Chang, Y. Zhao, H. Zheng, C. Dang, A review of loop heat pipes for aircraft anti-icing applications, *Appl. Therm. Eng.* 130 (2018) 528–540. doi:10.1016/j.applthermaleng.2017.11.030.
- [13] M. Bernagozzi, S. Charmer, A. Georgoulas, I. Malavasi, N. Michè, M. Marengo, Lumped parameter network simulation of a Loop Heat Pipe for energy management systems in full electric vehicles, *Appl. Therm. Eng.* 141 (2018) 617–629. doi:10.1016/j.applthermaleng.2018.06.013.
- [14] D.C. Mo, N. Ding, S.S. Lu, Gravity effects on the performance of a flat loop heat pipe, *Microgravity Sci. Technol.* 21 (2009) 95–102. doi:10.1007/s12217-009-9144-6.
- [15] L. Bai, G. Lin, H. Zhang, D. Wen, Effect of evaporator tilt on the operating temperature of a loop heat pipe without a secondary wick, *Int. J. Heat Mass Transf.* 77 (2014) 600–603. doi:10.1016/j.ijheatmasstransfer.2014.05.044.
- [16] W. Deng, Z. Xie, Y. Tang, R. Zhou, Experimental investigation on anti-gravity loop heat pipe based on bubbling mode, *Exp. Therm. Fluid Sci.* 41 (2012) 4–11. doi:10.1016/j.expthermflusci.2012.01.030.
- [17] M.N. Nikitkin, W.B. Bienert, K.A. Goncharov, Non condensable gases and loop heat pipe operation, *SAE Tech. Pap.* (1998). doi:10.4271/981584.
- [18] P. Prado-Montes, D. Mishkinis, A. Kulakov, A. Torres, I. Pérez-Grande, Effects of non condensable gas in an ammonia loop heat pipe operating up to 125 C, *Appl. Therm. Eng.* 66 (2014) 474–484. doi:10.1016/j.applthermaleng.2014.02.017.
- [19] J. He, G. Lin, L. Bai, J. Miao, H. Zhang, Effect of non-condensable gas on the operation of a loop heat pipe, *Int. J. Heat Mass Transf.* 70 (2014) 449–462. doi:10.1016/j.ijheatmasstransfer.2013.11.043.
- [20] A.R. Anand, Investigations on effect of noncondensable gas in a loop heat pipe with flat evaporator on deprime, *Int. J. Heat Mass Transf.* 143 (2019) 118531. doi:10.1016/j.ijheatmasstransfer.2019.118531.
- [21] H. Wang, G. Lin, X. Shen, L. Bai, D. Wen, Effect of evaporator tilt on a loop heat pipe with non-condensable gas, *Int. J. Heat Mass Transf.* 128 (2019)

- 1072–1080. doi:10.1016/j.ijheatmasstransfer.2018.09.033.
- [22] R. Singh, A. Akbarzadeh, M. Mochizuki, Operational characteristics of the miniature loop heat pipe with non-condensable gases, *Int. J. Heat Mass Transf.* 53 (2010) 3471–3482. doi:10.1016/j.ijheatmasstransfer.2010.04.008.
- [23] W. Joung, K.S. Gam, Y.G. Kim, I. Yang, Hydraulic operating temperature control of a loop heat pipe, *Int. J. Heat Mass Transf.* 86 (2015) 796–808. doi:10.1016/j.ijheatmasstransfer.2015.03.056.
- [24] R. Yang, G. Lin, J. He, L. Bai, J. Miao, Investigation on the effect of thermoelectric cooler on LHP operation with non-condensable gas, *Appl. Therm. Eng.* 110 (2017) 1189–1199. doi:10.1016/j.applthermaleng.2016.09.050.
- [25] K.R. Wrenn, D.A. Wolf, E.J. Krolczek, Effect on noncondensable gas and evaporator mass on Loop Heat Pipe performance, *SAE Tech. Pap.* (2000). doi:10.4271/2000-01-2409.
- [26] C. Baker, D. Butler, E. Grob, P. Jester, Geoscience laser altimetry system (GLAS) loop heat pipe anomaly and on orbit testing, in: 41st Int. Conf. Environ. Syst. 2011, ICES 2011, American Institute of Aeronautics and Astronautics, Reston, Virginia, 2011: pp. 1–10. doi:10.2514/6.2011-5209.
- [27] T.T. Hoang, W.J. Armiger, R.W. Baldauff, B.N. Nguyen, D.R. Mahony, W.C. Robinson, Performance of COMMX loop heat pipe on TacSat 4 spacecraft, 42nd Int. Conf. Environ. Syst. 2012, ICES 2012. (2012) 1–9. doi:10.2514/6.2012-3498.
- [28] J. Baumann, B. Cullimore, B. Yendler, E. Buchan, Noncondensable gas, mass, and adverse tilt effects on the start-up of loop heat pipes, *SAE Tech. Pap.* (1999). doi:10.4271/1999-01-2048.
- [29] L. Bai, G. Lin, H. Zhang, Experimental study on steady-state operating characteristics of gravity-assisted loop heat pipes, *Hangkong Xuebao/Acta Aeronaut. Astronaut. Sin.* 29 (2008) 1112–1117.
- [30] L. Bai, J. Guo, G. Lin, J. He, D. Wen, Steady-state modeling and analysis of a loop heat pipe under gravity-assisted operation, *Appl. Therm. Eng.* 83 (2015)

- 88–97. doi:10.1016/j.applthermaleng.2015.03.014.
- [31] P.Y.A. Chuang, J.M. Cimballa, J.S. Brenizer, Experimental and analytical study of a loop heat pipe at a positive elevation using neutron radiography, *Int. J. Therm. Sci.* 77 (2014) 84–95. doi:10.1016/j.ijthermalsci.2013.10.010.
- [32] A.A. Chehade, H. Louahlia-Gualous, S. Le Masson, I. Victor, N. Abouzahab-Damaj, Experimental investigation of thermosyphon loop thermal performance, *Energy Convers. Manag.* 84 (2014) 671–680.
doi:10.1016/j.enconman.2014.04.092.
- [33] J. He, J. Miao, L. Bai, G. Lin, H. Zhang, D. Wen, Effect of non-condensable gas on the startup of a loop heat pipe, *Appl. Therm. Eng.* 111 (2017) 1507–1516. doi:10.1016/j.applthermaleng.2016.07.154.